Journal of The Electrochemical Society, **162** (14) A2646-A2650 (2015)
0013-4651/2015/162(14)/A2646/5/$33.00 © The Electrochemical Society

Lithium Plating on Graphite Negative Electrodes: Innovative Qualitative and Quantitative Investigation Methods

Claudia Birkenmaier,[a,b] Bernhard Bitzer,[c] Matthias Harzheim,[d,e] Andreas Hintennach,[a,z] and Thomas Schleid[b]

[a]*Daimler AG, HPC G012, Böblingen 71034, Germany*
[b]*Institute for Inorganic Chemistry, University of Stuttgart, Stuttgart 70569, Germany*
[c]*Daimler AG, HPC U028, Ulm 89081, Germany*
[d]*Daimler AG, HPC H152, Stuttgart 70367, Germany*

The effect of metallic lithium depositing on the negative electrode surface of a carbon-based lithium-ion battery instead of intercalating into the graphitic layers, namely lithium plating, can be assigned to charging at low temperatures and/or high currents. Cell parameters, such as performance and safety, are negatively influenced by this phenomenon. Elemental lithium deposited on the negative electrode requires more space than the intercalated compound and therefore increases the cell volume. Thus, the thickness changes during cycling can be used as a qualitative indicator for lithium plating. In this context, two different non-destructive experimental setups detecting the thickness profiles in situ are presented. Moreover, a quantitative titration technique to determine the exact amount of lithium deposited is established.

Manuscript submitted June 16, 2015; revised manuscript received September 23, 2015. Published October 2, 2015.

The utilization of lithium-ion batteries (LIBs) in automotive applications requires extended cycle life and prolonged calendar life. Therefore, the investigation of their capacity-fading mechanisms is of increasing interest.[1] Carbon-based materials, in particular graphites, are commonly used as negative electrodes in these energy storage systems.[2,3] Thus, most studies regarding negative electrode-aging mechanisms were conducted with graphite-based cells.[4] Mechanisms, such as cracking of particles due to volume changes, decomposition of the binder, growth of the solid electrolyte interface (SEI), and metallic lithium deposition are primarily influences on the aging process of an negative electrode.[5] The latter degradation process, also known as lithium plating, is usually formed as a consequence of charging at low temperatures, high state of charge (SOC) and high charge rates.[6] These conditions lead to a polarized negative electrode and poorer electrode kinetics. As soon as the potential of the negative electrode falls below 0 V measured versus the Li/Li^+ half cell, lithium plating is thermodynamically favored on the negative electrode surface.[6,7] The structure of deposited lithium depends on the current applied.[8] Orsini et al. have demonstrated that lithium deposition on metallic electrode surfaces generally has a mossy structure through low-current charging, whereas high-charge rates lead to dendrites.[8,9] Lithium dendrites, which occur on graphite as well, have a serious effect on the cell's safety and performance issues. The dendrites, which grow directly on the negative electrode, can cause short circuits, leading to serious fire hazards associated with the flammable organic electrolyte.[6,10,11]

State of the Art Characterization of Lithium Plating Behavior

Depending on the effect they rely on, today's methods for detecting lithium plating can be distinguished into three categories:

(i) Detection of the negative electrode potential vs. Li/Li^+, e.g. in half cells or with a reference electrode,
(ii) Electrical measurements of plating phenomena, such as loss of capacity or rise of internal resistance,
(iii) Physical and chemical treatment for post mortem-analysis, e.g. titration.

Currently, the detection of lithium plating is conducted via measuring the negative electrode potential (method (i)) either in half cells or a built-in reference electrode. The reference electrode can influence the measurement negatively by affecting the electrode processes.[12,13] In the case of a large-scale production, measuring the negative electrode potential is not an option for the characterization of unmodified cells.

Method (ii) implies the determination of plating by mapping the maximum charge current at different operating conditions, while the degradation performance is checked. Here, the detection of the cell's capacity is the parameter of choice, because of the direct correlation between cell capacity and loss of active lithium.

In order to gain further insight into the degradation processes, a post-mortem analysis can be conducted (method (iii)). The variety of chemical and physical analytical tests is not discussed further in this article.

Principles

During the cycling process, lithium cations are reversibly intercalated in the spaces between the graphite basal planes. The resulting solid solutions have compositions from an unlithiated state to a maximum lithiation of LiC_6. The uptake to the fully-lithiated state is accompanied by a volume expansion of up to 10%, which induces mechanical stress on the negative electrode material.[14] Owing to a small contribution of the positive electrode's volume change, the overall alteration in cell thickness during cycling originates from the negative electrode.[15,16]

Moreover, a change in porosity, gas evolution or irreversible reactions can lead to a remaining increase of the overall cell volume.[16–18] A significant increase in the cell volume during formation is also described in reference.[19] In the case of lithium plating, there is an additional increase in thickness during the charging process. This results from the overall volume of carbon and lithium separately being larger than of fully-lithiated LiC_6.[17] Measuring changes in volume can therefore be an effective method for determining lithium plating.

Theoretically, the cell volume expands by 0.37 cm^3 for the amount of lithium providing a charge of 1 Ah. This value can be calculated from the molar volume of metallic lithium (V_m) minus the volume change of the graphite layer, if the cations were intercalating instead of depositing. This theoretical assumption implies a flat and homogeneous lithium deposition on the negative electrode. In fact, the deposition exhibits a mossy or dendritic structure and therefore exceeds this theoretical value.

According to the inhomogeneity of the cell, there are areas, in which plating is favored. For instance, many cells tend to begin with plating in a thin line near the cell edge (Fig. 1). This inhomogeneity results from production, temperature and edge or boundary effects.

If the cell expansion is measured with a limited number of measurement points, thus their locations must be chosen very carefully. Compared to the entire cell surface, the areas, in which plating starts are very small. Thus, there is a high risk of choosing a measurement

[e]Present address: Fliegenstraße 5, Munich 80337, Germany.
[z]E-mail: andreas.hintennach@daimler.com

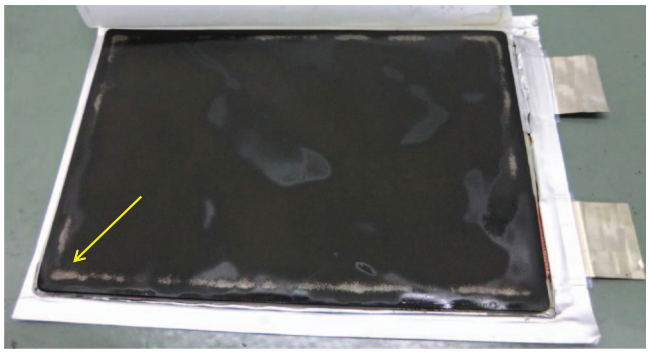

Figure 1. Lithium plating at the edge area due to cell inhomogeneities (cell size: 128 mm × 196 mm).

point, where no plating occurs at first. In order to minimize the possibility of this failure, post-mortem analysis to detect the plated area prior to thickness measurements, must be conducted.

To exclude the possibility of setting the wrong measurement point and avoid post-mortem analysis, the entire surface must be scanned. The implementation of an appropriate measurement device is described in next section.

The reaction of lithium and electrolyte causes the evolution of gas, which further increases the cell volume. This does not affect the method, because at low temperatures, this reaction can be primarily ascribed to the effect of plating, which further amplifies the measured expansion.

The expansion of active materials has already been discussed in the literature. However, most papers concerning this, address cell aging by way of the induced mechanical stress on the particles. This is accomplished either in experimental work[2,18,20–24] or modeling.[21,25,26]

Only a few papers describe measurements on volume changes of complete cells, either through directly measuring the change in cell thickness with linear voltage displacement transducers (LVDTs)[19,21,27] or thickness gauges,[17,22,28] or measuring changes of strains in a framework, which constrains the cells.[29,30] While the papers show conclusive data about the graphite-driven, non-linear cell expansion as a function of lithiation, none of them take local differences in the cell surface into concern.

Development of Functionality of the Laser Triangulation Setup

In order to track changes in the surface morphology of the entire cell, the measurement setup must provide a large amount of measurement points. To evaluate the change in thickness due to charging or lithium plating, the setup must meet a high demand with respect to accuracy, which is in the range of a few micrometers. For this purpose, a laboratory instrument based on a high-precision laser triangulation sensor was developed. A laser beam is focused on the anode surface. The angle of the reflecting beam is measured by this sensor. Knowing the distance between sensor and laser-diode as well as the angle of the reflected beam, the distance to the reflecting surface can be calculated via triangulation. The rated accuracy is about 1.5 µm. The sensor can be moved over the entire cell area by a two-axis positioning system. The high-precision ball screw steel axes are driven by two stepper motors. Based on an ARM Cortex M4, a motor controller has been developed that controls the axis movements on the one hand and the laser triangulation sensor on the other. This system enables the sensor to be triggered at a defined position. The motor controller calculates the optimum acceleration and deceleration ramps of the two axes for each part of the motion, to achieve a minimal deviation from the desired scanning path. To initialize the system, a reference measurement of the surface must be taken, which serves to correct the data recorded later. The motor and laser controller communicate via a serial interface with the control personal computer (PC). The setting of measurement parameters and subsequent visualization of the results are accomplished by software especially developed for this purpose.

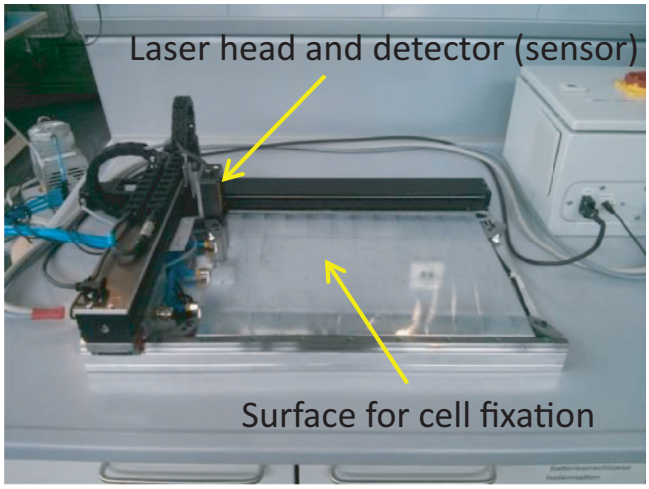

Figure 2. Measurement setup for in situ cell thickness measurements.

The measurement setup is shown in Figure 2.

Experimental

In the following experimental part, the detection of lithium plating via cell-thickness measurement was conducted. In preliminary tests, the cell behavior was investigated using the standard method described in Ref. 17 with a single measurement point. Based on these results, measurements with the laser triangulation tool were conducted. The cell used for all experiments in this paper is a 20 Ah pouch cell with a NMC positive electrode and a graphite negative electrode.

Preliminary tests using a single measurement point.— With the setup described in Ref. 17, an estimation of the maximum charge current for the cell was conducted. The arrangement is based on measuring the cell thickness with a dial indicator in one discrete point on the cell surface. As long as the charge current is below a specific limit, all cycles show the same thickness profile without any irreversible gain in cell thickness. After exceeding this current limit a remaining thickness increase can be detected after every cycle.

For evaluating the reproducibility of the experiment and determining possible influences of gas evolution, the test cell was cycled for 150 times measuring the cell thickness at one single point in the center of the cell. The parameters were 25°C at a charge rate of 20A = 1C. The progression of the cell thickness at the end of the discharging step of each cycle is shown in Figure 3. Note that the graph shows the change in thickness not its absolute value.

As Figure 3 shows the repeatability is in the range of only a few micrometers. This means that cycling under standard conditions does not lead to an irreversible increase in the overall cell thickness. Thus there is no gas evolution under these conditions.

Paper[17] describes an experiment for the distinction of thickness changes between gas evolution and plating. There, two measuring points are measured simultaneously. At one of the points an additional pressure pushes on the surface suppressing possible gas. In case of gas evolution the measurement point without external pressure would show much larger expansion. This experiment was reproduced. As a result, the test cell showed again no significant influence on the cell thickness by gas evolution, at least over a limited number of cycles with Li-plating.

For evaluating the plating conditions, the cell is cycled from 40 to 60% (=20% Δ SOC) applying different charge currents. In Figure 4, the thickness profile of the cell during cycling is shown, which depicts a strong increase in the overall thickness. Consequently, the maximum charge current is exceeded and lithium cations are

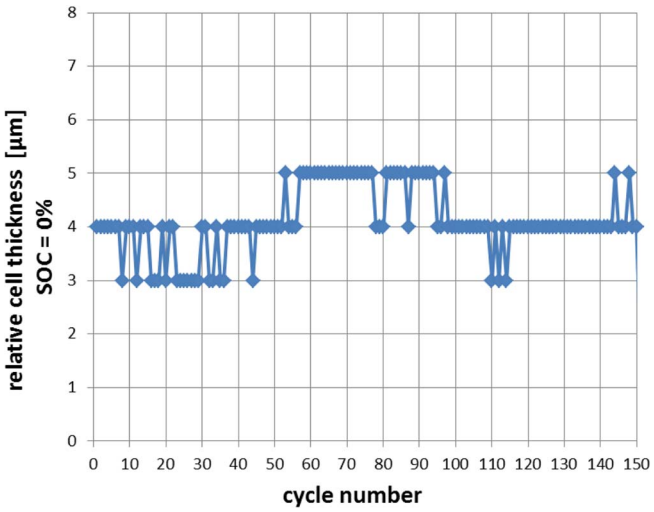

Figure 3. Change in cell thickness during charging without lithium plating. Measurement parameters were T = 25°C and a charging rate of 20A.

depositing on the negative electrode as metal. A subsequent cell opening revealed massive plating, which confirmed this assumption.

Measurement procedure with the laser triangulation setup.— The entire procedure consists of two sets of 20 cycles each. In the first set, charged with 10 A, only minimal plating should take place. In the second set, charged with 15 A, significant plating is expected. A short relaxation time of 5 minutes is provided after each charge or discharge step and the discharge current is constantly held at 5 A. The charge or discharge profile is constant current and stopped when the charge reached 4 Ah. The entire setup is placed in a climate chamber at an ambient temperature of 0°C.

The measurement covers a line 5 mm next to the long side of the cell's edge. The results of previously conducted experiments showed, that under these conditions plating starts there, see Principles section.

Results and Discussion

The measured voltage profile is displayed in Figure 5. The voltage peaks during the 15 A charge and 5 A discharge are significantly rising, which is due to cell degradation, e.g. the rise of the internal resistance (Ri) through lithium plating. This is consistent with the results in Preliminary tests using a single measurement point section. At 10 A cycles, there is only slight plating, which has only little effect on the voltage profile.

Laser triangulation measurements.— In the experiment, the cell thickness throughout a line parallel to the cell's edge is conducted

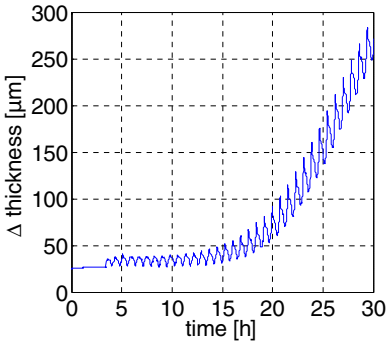

Figure 4. Cell thickness during cycling at 0°C, at 15 A charging current and 5 A discharging current from 40 – 60% SOC.

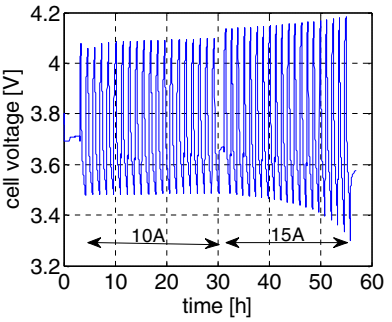

Figure 5. Cell voltage during the cycling at a temperature of 0°C and a charging rate of 10 and 15A.

every six minutes. For displaying the average gain in cell thickness, the arithmetic mean value of each measurement set is plotted as a function of time (see Fig. 6). The small periodical thickness changes hereby reflect the reversible intercalation of lithium into graphite. During the low-current profile, there is only a slight offset increase notable, which means that the lithium plating occurring is largely reversible. Increasing the current to 15 A, however, leads to a massive deposition of metallic lithium on the negative electrode. This induces an increase in the overall cell thickness. Moreover, the amplitude of the periodical thickness change is larger, because of the higher amount of reversibly deposited lithium.

During the first set of cycles with minimal plating, the offset is constantly rising with every cycle, leading to a persistent amount of deposited lithium. At the high current cycles, the slope and, thus the cell degradation, are rising. The remaining active surface area decreases with every charging procedure, leading to a higher area-specific current or more plating.

For demonstration of the progress in thickness increase, a video is added in the supplementary information.

Giving an insight in local differences, Figure 7 plots the surface structure of the 5th cycle in Figure 6 during charging (a) and discharging (b). The dilatation of the cell is mostly uniform, which is shown through the parallel translation of the cell thickness profile during charging as well as during discharging. Moreover, the characteristic of the thickness profile is maintained. Figures 7c and 7d displays the 7th of the high-current cycles from Figure 6. The overall increase in thickness is much higher in comparison to the cycles at 10 A.

The plot in Figure 8 shows the range from 60 to 100 mm in Figure 7 (highlighted in red) in detail. In the third axis the change in thickness over the time is shown. At the position of about 238 mm in the scale of Figure 8, a second peak arises next to the one, which has already been there during the low-current cycling. The peaks are probably caused by the evolution of dendrites or locally defined gas bubbles. During discharge, the overall thickness decrease is much higher, indicating the relevance of the reversible part of lithium plating. Noticeable during discharge the second peak is nearly completely vanishing.

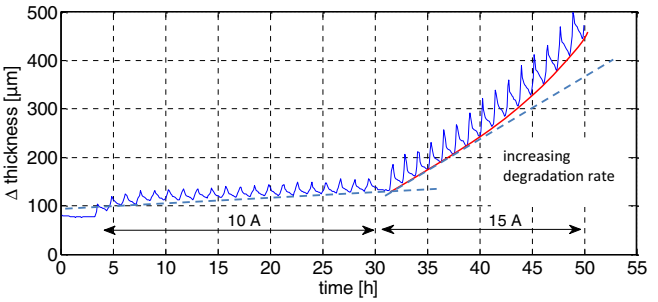

Figure 6. Arithmetical average of the cell thickness (parameters: T = 0°C and a charging rate of 10 and 15A).

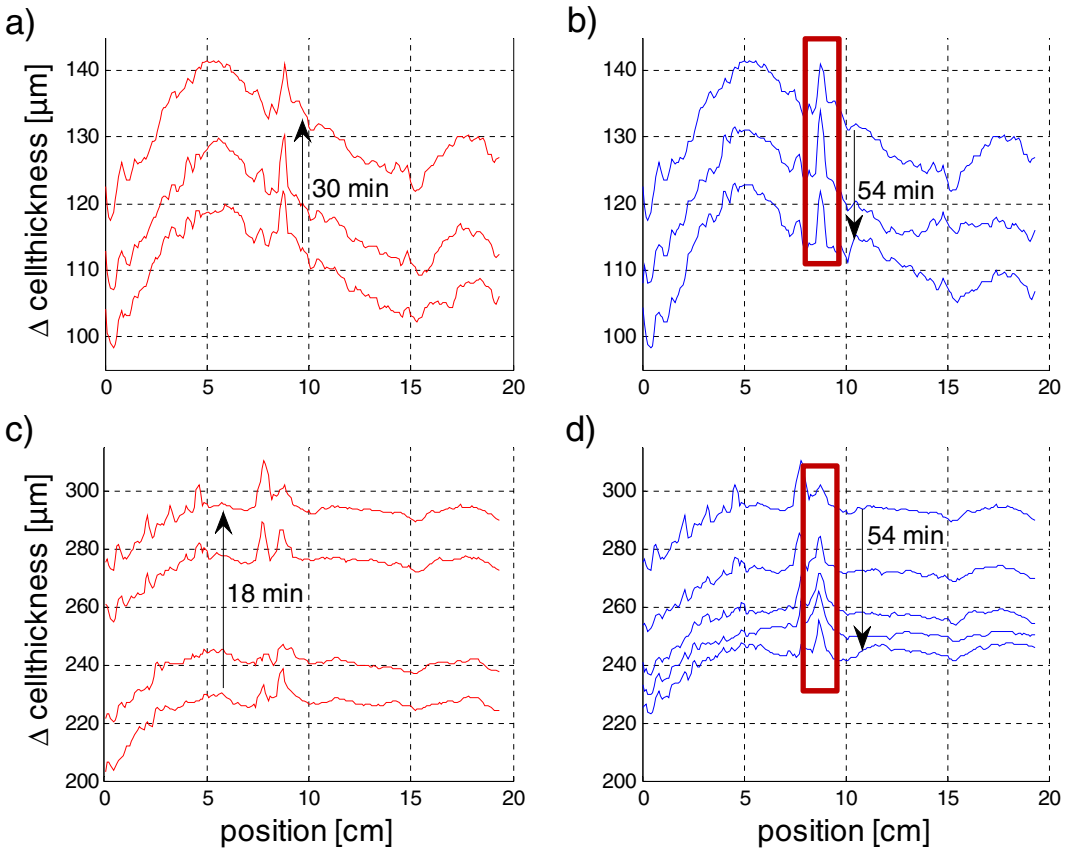

Figure 7. Thickness profile during charging (a, c) and discharging (b, d). Measurement was conducted at 0°C and a charging rate of 15A and a discharging rate of 5A.

Note that the scale changes from (7a, 7b) to (7c, 7d).

Local differences in expansion over the surface are in the region of <20 µm, which is small compared to the total change in cell thickness. Therefore, to gain the data for Figure 7, an arithmetic mean value was calculated and subtracted from each profile. Moreover, the initial thickness profile was further subtracted from all following data sets. This enables the possibility to visualize local inhomogeneity effects. After 40 h, for example, a significantly larger expansion can be observed in only a limited area (see arrow in Figure 8) while the rest shows less thickness increase. The evolution of a dendrite or gas bubbles in this region is a possible explanation for this. For better visualization, only part of the data is shown in the 3D plot of Figure 8.

Note that this procedure is only adaptive for Pouch-Cells since in prismatic cells thickness changes are caused by internal pressure rise.

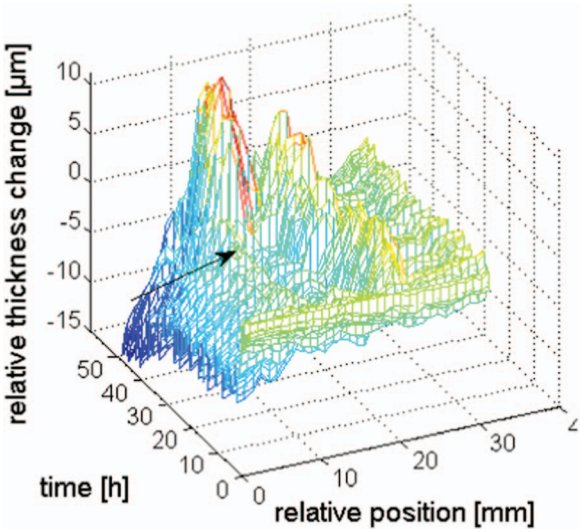

Figure 8. Relative change of the cell thickness with offset correction.

Chemical confirmation of lithium plating by titration method.— The thickness increase as a proof of plating does not provide information about the amount of deposited metallic lithium on the negative electrode surface. Therefore, a new method to determine this lithium amount by adding organic compounds, which selectively graft the metallic lithium parts was established. A similar method for a selective surface modification was already established in Ref. 31.

2-Desoxy-2-(3-methyl-3-nitroso-ureido)-D-glucopyranose was used for the selective modification of the plated surfaces of electrodes after electrochemical cycling. All chemicals were used as received from Sigma Aldrich without a precedent purification step. A solution of 2-Desoxy-2-(3-methyl-3-nitroso-ureido)-D-glucopyranose in dimethyl carbonate DMC (1 M) was prepared in an argon-filled glove box. Approximately 2 wt% of a solution of predispersed surfactants (Triton X-109, Triton X-209; 1:1 by volume) in ethylene carbonate:dimethyl carbonate (EC:DMC, 1:1 by volume, 10 wt%) was added under stirring. This solution could be directly added with a syringe between the electrodes into the electrolyte. Since the surface modification needs to result in a homogeneous coating of lithium plated parts of the electrode, it proved to be essential to adjust the stoichiometry with a slight excess of the additives used for selective surface reactions of the analyzed electrodes. For a homogeneous mixing of the additives with the electrolyte and to ensure a homogeneous wetting of the electrodes, it proved to be important to allow a standing time of about 30 minutes after the injection of the

2-Desoxy-2-(3-methyl-3-nitroso-ureido)-D-glucopyranose solution. An adjacent heating step (38 C, 15 min) initiated the irreversible surface modification. Note that no electrochemical cycling was performed after the additives were added. The used chemicals are stable at all open circuit potentials, so that a safe and homogeneous complex-coating of the lithium-plated areas on the surface is ensured. A few milliliters of the electrolyte were extracted with a syringe and analyzed via Inductively Coupled Plasma (ICP) to determine the lithium content. The same cell type was plated which led to an overall thickness increase of 39 µm. The ICP detected that 4.21% of the cell's overall lithium content deposited on the negative electrode surface. Note that there is no direct correlation between the amount of plated lithium and the thickness increase. This is because the volume expansion heavily depends on the plating morphology, which is influenced by current, temperature and material characteristics.

Comparison of the methods.— Measuring the thickness with a small amount of measuring points is an effective method for determining the operating window of a lithium-ion pouch-cell, although it implicates the risk of setting the points on locations, where plating starts delayed. To eliminate this risk, the entire cell surface can be measured with a 3D measuring setup as described in Development of functionality of the laser triangulation setup section.

Since the correlation between the thickness increase and the amount of deposited lithium differs with the cycle profile and the cell parameters, no direct conclusion on the amount of plating can be drawn. If the exact amount of deposition is of importance, a titration reaction with 2-Desoxy-2-(3-methyl-3-nitroso-ureido)-D-glucopyranose can be conducted, as described in Chemical confirmation of lithium plating by titration method section.

Conclusions

Lithium plating leads to an increase in the overall cell volume of carbon-based lithium-ion batteries. This phenomenon has been used in the literature to detect its occurrence. All previously conducted measurements discussing cell expansion only used a single measurement variable to quantify this effect. This only insufficiently takes existing cell inhomogeneity into account.

The onset of lithium plating occurs in discrete spots on the negative electrode surface. For an exact determination of the beginning of lithium plating, the entire cell surface must be measured. Therefore, a laser triangulation-based setup was developed enabling a precise surface-resolved thickness measurement. Using this setup, the plating behavior of a 20 Ah NMC pouch cell was analyzed. The measurement revealed significant local differences in expansion which results from inhomogeneity. Applying only few cycles this method enables a fast determination of the operation window of a pouch-cell. Thus no post-mortem analysis cell opening or severe damaging is necessary.

Moreover, the exact amount of deposited lithium was determined using a titration method.

References

1. M. Wohlfahrt-Mehrens, C. Vogler, and J. Garche, *Journal of Power Sources*, **127**, 58 (2004).
2. V. A. Sethuraman, L. J. Hardwick, V. Srinivasan, and R. Kostecki, *Journal of Power Sources*, **195**, 3655 (2010).
3. C. Wang, A. J. Appleby, and F. E. Little, *Journal of Electroanalytical Chemistry*, **497**, 33 (2001).
4. J. Vetter, P. Novák, M. R. Wagner, C. Veit, K. C. Möller, J. O. Besenhard, M. Winter, M. Wohlfahrt-Mehrens, C. Vogler, and A. Hammouche, *Journal of Power Sources*, **147**, 269 (2005).
5. N. Legrand, B. Knosp, P. Desprez, F. Lapicque, and S. Raël, *Journal of Power Sources*, **245**, 208 (2014).
6. M. Petzl and M. A. Danzer, *Journal of Power Sources*, **254**, 80 (2014).
7. R. Chandrasekaran, *Journal of Power Sources* **2014**.
8. F. Orsini, A. du Pasquier, B. Beaudouin, J. M. Tarascon, M. Trentin, N. Langenhuizen, E. de Beer, and P. Notten, *Journal of Power Sources*, **81–82**, 918 (1999).
9. F. Orsini, A. Du Pasquier, B. Beaudoin, J. Tarascon, M. Trentin, N. Langenhuizen, E. De Beer, and P. Notten, *Journal of Power Sources*, **76**, 19 (1998).
10. R. Bhattacharyya, B. Key, H. Chen, A. S. Best, A. F. Hollenkamp, and C. P. Grey, *Nature Materials*, **9**, 504 (2010).
11. L. Gireaud, S. Grugeon, S. Laruelle, B. Yrieix, and J. M. Tarascon, *Electrochemistry Communications*, **8**, 1639 (2006).
12. D. W. Dees, A. N. Jansen, and D. P. Abraham, *Journal of Power Sources*, **174**, 1001 (2007).
13. A. N. Jansen, D. W. Dees, D. P. Abraham, K. Amine, and G. L. Henriksen, *Journal of Power Sources*, **174**, 373 (2007).
14. A. Mukhopadhyay and B. W. Sheldon, *Progress in Materials Science*, **63**, 58 (2014).
15. J. R. Dahn, *Physical Review B*, **44,17**, 9170 (1991).
16. J. H. Lee, H. M. Lee, and S. Ahn, *Journal of Power Sources*, **119–121**, 833 (2003).
17. B. Bitzer and A. Gruhle, *Journal of Power Sources*, **262**, 297 (2014).
18. Y. Qi and S. J. Harris, *Journal of The Electrochemical Society*, **157**, A741 (2010).
19. N. M. Tsutomu Ohzuku and Sawai Keijiro, *Journal of Power Sources*, 73 (2001).
20. N. Zhan and H. Tang, *Journal of Power Sources*, **218**, 52 (2012).
21. R. Fu, M. Xiao, and S.-Y. Choe, *Journal of Power Sources*, **224**, 211 (2013).
22. M. Majima, T. Tada, S. Ujiie, E. Yagasaki, S. Inazwawa, and K. Miyazaki, *Journal of Power Sources*, **81–82**, 877 (1999).
23. J. Cannarella and C. B. Arnold, *Journal of Power Sources*, **269**, 7 (2014).
24. V. A. Sethuraman, M. J. Chon, M. Shimshak, V. Srinivasan, and P. R. Guduru, *Journal of Power Sources*, **195**, 5062 (2010).
25. J. Christensen and J. Newman, *Journal of Solid State Electrochemistry*, **10**, 293 (2006).
26. P. M. Gomadam and J. W. Weidner, *Journal of The Electrochemical Society*, **153**, A179 (2006).
27. J. Barker, *Electrochemica Acta*, **45**, 235 (1999).
28. H. M. L. Jae Hyun Lee and Ahn Soonho, *Journal of Power Sources*, 833 (2003).
29. X. Wang, Y. Sone, G. Segami, H. Naito, C. Yamada, and K. Kibe, *Journal of The Electrochemical Society*, **154**, A14 (2007).
30. J. Cannarella and C. B. Arnold, *Journal of Power Sources*, **245**, 745 (2014).
31. T. Mitsch, Y. Krämer, J. Feinauer, G. Gaiselmann, H. Markötter, I. Manke, A. Hintennach, and V. Schmidt, *Materials*, 4455 (2014).